

MASTER

CONF-790622--3

COMPTON SCATTERING OF PHOTONS FROM ELECTRONS IN
MAGNETICALLY INSULATED TRANSMISSION LINES*

K. L. Brover and J. P. VanDevender

Sandia Laboratories, Albuquerque, New Mexico 87185

Abstract

Self-magnetically insulated transmission lines are used for power transport between the vacuum insulator and the diode in high current particle accelerators. Since the efficiency of the power transport depends on the details of the initial line geometry, i.e., the injector, the dependence of the electron canonical momentum distribution on the injector geometry should reveal the loss mechanism. We propose to study that dependence experimentally through a Compton scattering diagnostic. The spectrum of scattered light reveals the electron velocity distribution perpendicular to the direction of flow. The design of the diagnostic is in progress. Our preliminary analysis is based on the conservation of energy and canonical momentum for a single electron in the \vec{E} and \vec{B} fields, determined from 2-D calculations. For the Mite¹ accelerator with power flow along Z , the normalized canonical momentum, μ , is in the range $-0.7 < \mu \leq 0$. For $k_x \parallel \hat{y}$, and $k_y \parallel \hat{x}$, our analysis indicates that the scattered photons have $1.1 \text{ eV} \leq h\nu_s < 5.6 \text{ eV}$ for ruby laser scattering and calculated with PH cubes.

Introduction

Self-magnetically insulated transmission lines are being developed for power transport in the particle beam fusion accelerator EBFA at Sandia. The efficiency of power and energy transport is sensitive to variations in line geometry which occur at the input and output convolutes. In this paper we consider how the dynamics of electron flow might be probed by Compton scattering. The evaluation has several steps. First, the distributions of the electric and magnetic fields in the EBFA self-magnetically insulated line² are inferred from simulations⁴ and 1-D theory.³ Then the relationship between the energy of a photon scattered from an electron with an axial canonical momentum P_z is calculated at various positions in the electron flow, for the \vec{E} and \vec{B} fields from the 2-D simulations and for those from the 1-D theory. A comparison of the two relationships illustrates the sensitivity of the diagnostic to the model for \vec{E} and \vec{B} . The particle trajectories for an assumed distribution of canonical momentum P_z in the axial direction are then calculated at a given position in the vacuum gap. Finally, the spectrum of scattered photons

for two different assumed canonical momentum distributions are calculated to illustrate the diagnostic. Each step will be examined in turn.

Electromagnetic Field Calculations

The triplate transmission line which is being incorporated into EBFA is represented by an equivalent coaxial transmission line with $r_c = 0.07 \text{ m}$ and $r_a = 0.08 \text{ m}$. This coax and the basic features in the Compton scattering experiment are shown in Fig. 1. From simulations² of this coaxial line, the power flow is represented by a boundary current, I_B , of 243 kA and a total current, I_T , of 450 kA at $V_0 = 2.4 \text{ MV}$. The current $I_T = I_T - I_B = 207 \text{ kA}$ is carried by electrons in the vacuum gap between conductors. The \vec{E} and \vec{B} fields for this particular case have been calculated previously by Burgeron and Poukey with a 2-D electromagnetic particle simulation code.² The agreement between the experiment and the code results for V , I_T , and I_B are excellent. We have also calculated the \vec{E} and \vec{B} fields for these initial conditions from parapotential theory.³ We noticed that under these conditions of power flow the value of C_2 as calculated by Eqs. (29) and (36) in Creedon's paper³ were inconsistent. This theory requires self-consistency which we achieved by optimizing V_0 so that $V_0 = v_{0c}^2(\gamma_0 - 1)/c$ is 2.4505 MV instead of 2.4 MV. This

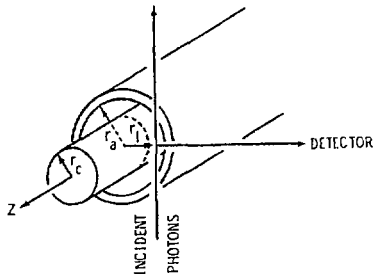


Fig. 1. Coax with basic features of Compton scattering experiment. Directions of electron power flow (I_T), incident photons, and detector are all mutually perpendicular.

*This work was supported by the U.S. Dept. of Energy, under Contract DE-AC04-76-DPO0789.

NOTICE
This report was prepared as an account of work sponsored by the United States Government. Neither the United States nor the United States Department of Energy, nor any of their employees, nor any of their contractors, subcontractors, or their employees, makes any warranty, express or implied, or assumes any legal liability or responsibility for the accuracy, completeness, or usefulness of any information, apparatus, product, or process disclosed, or represents that its use would not infringe privately owned rights.

DISTRIBUTION OF THIS DOCUMENT IS UNLIMITED

Fig

value of V_0 gives a self-consistent set of parameters V_0 , I_T , I_B , and Z_0 for parapotential theory and is well within experimental error in the measurements and the numerical fluctuations in the computational results. The \vec{E} and \vec{B} fields from 2-D calculations and the self-consistent (SC) parapotential theory are shown in Fig. 2.

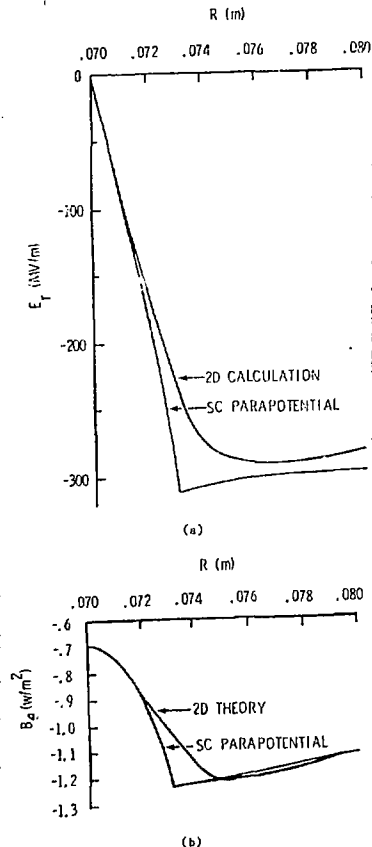


Fig. 2. Plot of \vec{E} and \vec{B} fields extrapolated from data points of Bergeron and Dzyubay² and according to SC parapotential³ theory.

The Photon Energy as a Function of Electron Canonical Momentum

In order to calculate the frequency of a Compton scattered photon, the velocity vector of the scattering electron needs to be known. From the conservation of energy and momentum for a single electron, Mendel⁴ has shown that

$$\gamma^2 \frac{V_r^2}{c^2} = [1 + \phi(r)]^2 - 1 - [\alpha(r) + \mu]^2 \quad (1)$$

where

$$\begin{aligned} V_r &\equiv \text{radial velocity component,} \\ \phi(r) &\equiv \text{normalized scalar} \\ &\quad \text{potential (= } e\psi/mc^2 \text{ with } \vec{E} = -\nabla\phi), \\ \alpha(r) &\equiv \text{Z-component of normalized vector} \\ &\quad \text{potential (= } eA_z(r)/mc \text{ with } \vec{E} = \nabla A), \\ \mu &\equiv \text{Z-component of normalized canonical} \\ &\quad \text{momentum (= } eV_z/mc \text{ with} \\ &\quad V_z = \frac{\gamma \hbar \omega}{c} + \frac{\hbar k_z}{2}, \text{ and} \\ \gamma &\equiv \frac{1}{\sqrt{1 - V^2/c^2}} = \frac{1}{1 + \phi(r)} \text{ (by energy} \\ &\quad \text{conservation)}. \end{aligned}$$

In Eq. (1) a new parameter, μ , is introduced which is the normalized canonical momentum.⁵ For steady-state electron flow in a transmission line in which $\partial/\partial Z \neq 0$, μ is a constant of the electron motion. If the electron originates from the cathode where $\phi = V_z = \alpha = 0$, then $\mu = 0$. Consequently, it is often assumed that $\mu = 0$ for all electrons in the flow. However, self-magnetically insulated transmission lines have a transition section between the weakly, electrically stressed vacuum insulator and the highly stressed line. In the transition section, $\partial/\partial Z \neq 0$ and μ is not a constant of motion. Consequently, electrons with $\mu \neq 0$ can be injected into the uniform line, and produce a distribution $F(\mu)$ with a finite width $\Delta\mu$, for the electron flow. It is thought that the detail structure in $F(\mu)$ determines the power transport in long, self-magnetically insulated lines,^{6,7} and the stability of the electron flow may be understood by studying $F(\mu)$ under various conditions. Stable orbits corresponding to solutions of Eq. (1) for which $V_r \geq 0$ in the gap can be found for various values of μ . In Fig. 3 we have plotted the radial positions of the lower and upper turning points for stable orbits as a function of μ . These results show that the orbits are very similar for scalar and vector potentials based on parapotential and 2-D calculations. We also see that for $\mu = 0$, the orbits are contained within the sheath⁸ and return to the cathode surface. Orbits with $\mu < 0$ have upper turning points beyond the sheath⁸ and tend to remain isolated from the cathode surface. The minimum μ corresponds to those orbits whose upper turning point just grazes the anode.

According to Compton scattering theory for the geometry shown in Fig. 1, the energy of the scattered photons, $\hbar\omega_s$, is related to $V(r_1, \mu)$ by the expression⁹

$$\hbar\omega_s = \frac{\hbar\nu_1}{1 - V(r_1, \mu)/c} \quad (2)$$

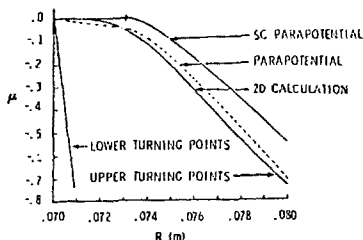


Fig. 3. Plot of μ vs. the position of lower and upper turning points. The dotted line was calculated by parapotential theory using same I_B , I_p , and V_0 as was used for 2-D calculation.

where r_p is the radial position of the incident laser beam in the gap. Scattered photon energies as a function of μ are plotted in Fig. 4 for various values of r_p with $h\nu_0 = 1.786$ eV from a ruby laser. The values of $V(r_p, \mu)$ needed in Eq. (2) were determined from Eq. (1) using potentials from 2-D calculations with $\mu_{lower} \leq \mu \leq \mu_{upper}$. These results indicate that for this geometry, optical detection is required.

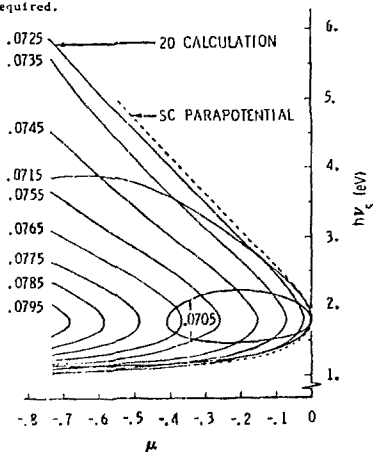


Fig. 4. Plot of scattered photon energies vs. μ for various positions for the fields from the 2-D computations and, of the laser probe beam. The dotted line has $h\nu_s(\mu)$ from the fields from the self-consistent parapotential calculation at $r_p = 0.0725$ m for comparison.

Calculated Spectra for an Assumed $F(\mu)$.

The number of scattered photons with energy between E , $E + dE$ is given by the expression

$$\frac{dN}{dE} = \frac{U I}{h\nu_0} \int_{r_1}^{r_2} D(r_p) F(\mu) \left| \frac{dr_p}{dE} \right|^{-1} \int_{\Omega} \frac{d\Omega}{4\pi} \quad (3)$$

where

- U = energy of incident laser pulse,
- l = interaction length of beam and electron plasma visible to the detector.
- $D(r_p)$ = number of electrons/m² at r_p from Ref. 2.
- $F(\mu)$ = fraction of electrons with normalized canonical momentum μ .
- $C(r_p, E)$ = normalized canonical momentum at some position in the gap, r_p , as a function of scattered photon energies (see Fig. 4), and
- $\frac{d\sigma}{d\Omega}$ = Compton differential scattering cross section.

In using Eq. (3) to calculate the scattered spectra, we assume the laser energy is 1 joule, the collector system subtends one steradian of solid angle, and the electron number density is 10^{18} m⁻³. For a uniform canonical momentum distribution, dN/dE versus E ($h\nu_s$) is plotted in Fig. 5 for several positions of the probing laser beam. The total number of scattered photons is also noted as N_s in these plots. We also assumed a Gaussian distribution, $\exp(-0.5(\mu - \mu_0)/\Delta\mu)^2$, with $\mu_0 = 0$ and $\Delta\mu = 0.1$; the results of the calculation using this distribution is plotted in Fig. 6.

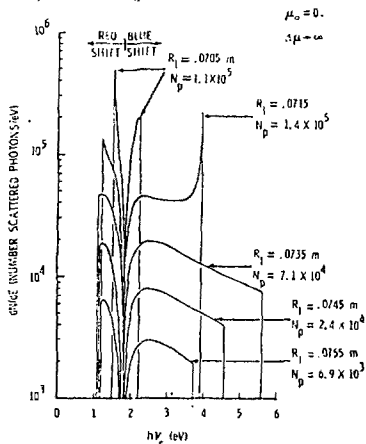


Fig. 5. Plot of dN/dE vs. $h\nu_s$ for uniform distribution in μ .

$$\mu_0 = 0.$$

$$\mu = -1$$

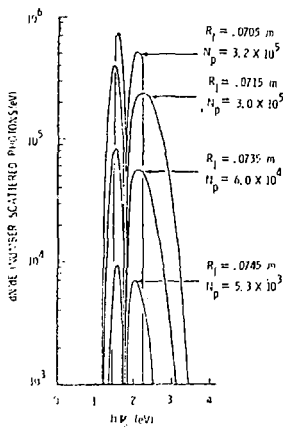


Fig. 6. Plot of dN/dE vs. $h\nu_s$ for Gaussian distribution in μ centered about $\mu_0 = 0$ with $\Delta\mu = 0.1$.

Discussion

In the proposed experiment to measure $F(\mu)$ in an EBFA-I self-magnetically insulated transmission line, the total number of collected photons will be $N_p \approx 10^5$. The photons will be in the visible region of the spectrum and they will be spectrally resolved with a grating and recorded with a photomultiplier and oscilloscope combination for each data channel. Assume that the spectrometer has a transmission efficiency $T_s = 0.2$, the photomultiplier has a quantum efficiency $\eta_{pm} = 0.03$ and a gain $G = 10^6$. If the data is recorded in a $\Delta t = 10$ ns pulse into $N_c = 5$ data channels, then the average signal into a 50 ohm oscilloscope will be

$$V = 50 \frac{N_p T_s \eta_{pm} G}{N \Delta t} = 0.6 \text{ volts}$$

which is easily recordable.

The functional relationship between $h\nu_s$ and μ features a reasonably strong correspondence of $F(h\nu_s)$ to $F(\mu)$ for the proposed experiment and the interpretation of the data is reasonably insensitive to the assumed model for the electromagnetic field distribution in the electron flow.

The electrons produce a bremsstrahlung x-ray pulse that will produce a signal on the detector. The scattered light can be optically delayed until the detector recovers from the x-ray pulse so the x-ray background can be tolerated.

The limiting factor to the Compton scattering diagnostic to measure $F(\mu)$ appears to be the background light from the plasma on the cathode. A significant amount of light can be expected, but no measurements have been made of its intensity or spectral distribution. The ratio of scattered light to plasma light improves as the bandwidth $\Delta\mu$ of the scattered light decreases. If the width $\Delta\mu$ of $F(\mu)$ is $\approx 10^{-2}$, as recent calculations have indicated, the scattered light has a wavelength spread of only 3 \AA , which would give a very favorable ratio of scattered light to plasma light.

Conclusion

The Compton scattering diagnostic is capable in principle of resolving the canonical momentum distribution $F(\mu)$ in self-magnetically insulated electron flow. The limiting factor is the ratio of background plasma light from the cathode plasma and the scattered light, which is strongly dependent on the width of $F(\mu)$ itself.

References

1. J. P. VanDevender, J. Appl. Phys. **50**, No. 6 (1979).
2. K. D. Bergeron and J. W. Poukey, Appl. Phys. Lett. **32**, 8 (1978).
3. J. N. Crendon, J. Appl. Phys. **46**, 2946 (1975).
4. C. W. Hendel, J. Appl. Phys. **50**, No. 7 (1979).
5. J. D. Jackson, Classical Electrodynamics (Wiley, NY, 1975), p. 574.
6. J. P. VanDevender, Proc. 2nd Int'l. Conf. on Pulsed Power, Lubbock, TX (1979).
7. Z. L. Nasa and J. P. VanDevender, same as Ref. 6.
8. G. Ward and R. E. Peckacek, Phys. Fluids **15**, 2202 (1972).